Regular Article

PHYSICAL CHEMISTRY RESEARCH
Published by the
Iranian Chemical Society
www.physchemres.org
info@physchemres.org

Phys. Chem. Res., Vol. 12, No. 2, 467-481, June 2024
DOI: 10.22036/pcr.2023.413995.2406

Elimination of Turbidity from a Maghnite Suspension by Coagulation/Flocculation Using a Copolymer Modified from N-vinyl Imidazole

C. Benouis[a], M.I. Ferrahi[a], R. Meghabar[a], B. Bouras[b], M. el Amine Zennaki[b,*] and H. Zerrigui[a]

[a]*Polymer Chemistry Laboratory, Oran 1 Ahmed Ben Bella University, Oran, Algeria*
[b]*Laboratory of Organic Electrolytes and Polyelectrolytes Application (LAEPO).*
Department of Chemistry, Faculty of Science, Tlemcen University, Algeria
(Received 30 August 2023, Accepted 17 October 2023)

In this work, N-vinyl imidazole (NVI) and glycidyl methacrylate (GMA) were combined to create poly(NVI-GMA). The synthesis of this novel cationic copolymer was initiated using high-temperature, ultraviolet (UV) radiation, and microwave radiation. The cationic level of poly(NVI-GMA) was optimized during the copolymerization process. The ideal synthesis conditions included a 2% initiator concentration, equal proportions of NVI and GMA (50% (v/v) each), a polymerization duration of 4 min, and an acidic pH reaction media. UV-visible, FTIR, and ^{1}H NMR techniques were employed to examine the structure of the copolymer. To investigate the flocculation performance of the highly cationic poly(NVI-GMA) in purifying water with high turbidity and to study and summarize the flocculation mechanism, several analyses including Fourier transform infrared (FTIR), X-ray diffraction (XRD), and thermogravimetric (TGA) analyses were conducted. Experimental simulations utilizing maghnite as a coagulant yielded a transmittance of 96.9% in the supernatant with a concentration of 6 mg l^{-1}, a brief stirring duration of 20 min, an acidic pH, and a stirring speed of 200 rpm.

Keywords: N-vinyl imidazole, Microwave, Copolymerization, Turbidity, Maghnite

INTRODUCTION

Global industrial development has experienced recent growth, resulting in a significant increase in water usage. Consequently, a considerable amount of wastewater is generated and discharged into the environment without proper treatment [1]. Industrial effluents exhibit varying concentrations of heavy metals, dyes, suspended particles, turbidity, salts, and sludge volume [2].

This wastewater contains colloids, which are finely dispersed solid particles with negative electric charges on their surfaces. These particles repel each other, thus remaining in suspension [3]. Due to their challenging removal through conventional physical techniques such as filtration or settling [2], the addition of chemicals to neutralize the charges on colloidal particles becomes necessary [4].

The discharge of highly turbid wastewater into the environment poses risks to aquatic life, obstructs light penetration, and degrades the quality of receiving water bodies [5,6]. Colloidal components in wastewater contribute to its turbidity, which can act as adsorption sites for hazardous compounds or result in unpleasant taste and odor [5]. Turbidity, a measure of water's cloudiness and haziness caused by suspended and colloidal particles (including organic, inorganic, and biological pollutants), is a significant concern in water treatment [7,8].

Various methods such as chemical precipitation [9], biological treatment [10], membrane filtration [11,12], photocatalysis [13], ion exchange resin [14], and coagulation/flocculation [15,16] are employed to remove turbidity, suspended solids, dissolved solids, and color from water and wastewater. Among these methods, coagulation/flocculation is a well-established technique in

*Corresponding author. E-mail: aminezen12@gmail.com

industrial wastewater pretreatment, as it effectively removes suspended particles [17].

The coagulation-flocculation process, widely used for industrial-scale wastewater treatment, becomes possible by adding coagulants. Coagulants act as agents that destabilize colloidal particles and delicate solid suspensions, allowing them to agglomerate under favorable conditions [18]. Inorganic coagulants (salts) and synthetic and natural organic polymers are commonly used coagulants added to wastewater to destabilize colloidal particles [19]. Natural coagulants are bio-extracts obtained from plants, seeds, marine crustacean and shellfish biomasses, and microbial organisms. They are generally safe, environmentally friendly, biodegradable, non-toxic, non-corrosive, and generate minimal sludge.

The coagulant used in this article is Maghnite. It is a bentonite from the Maghnia Tlemcen region. It is generally in the form of a mineral powder consisting essentially of montmorillonite clay (smectite family) [15]. Maghnite is used in many industrial fields, including pharmaceuticals, cosmetics, civil engineering, food processing, industrial waste, domestic waste, radioactive waste treatment, and the treatment of water contaminated with heavy metals [18].

The stable colloidal state of maghnite is due to the negative charge on the surface of the particles, which creates repulsive forces between the clay particles and eliminates the tendency of the particles to fuse and agglomerate. The negative charge is formed by a clay core surrounded by strongly bound O_2 and OH ions, around which a cloud of positive ions is formed by gravity, ensuring neutralization of the system (H+ and exchangeable cations). Negatively-charged particles repel each other and are deagglomerated to form a stable suspension. Otherwise, particles will aggregate and agglomerate to form an unstable suspension. Colloidal properties are very important for clay cleaning processes.

Poly N-vinyl imidazole is a readily available polycationic polymer with untapped potential. These materials offer several advantages, including easy availability, affordability, high biocompatibility, and chemical modifiability, allowing for copolymerization with other polymers. In this case, glycidyl methacrylate (GMA) was chosen as a monomer to obtain functionalized copolymers with diverse physicochemical properties, ranging from hydrophilic to hydrophobic solubilities. This characteristic provides a novel approach to quickly obtain amphiphilic block copolymers capable of self-organization into micelles [20], exhibiting excellent biocompatibility [21], without altering the morphological characteristics of GMA. In recent years, this amino polymer has garnered significant interest in water treatment processes for the removal of dissolved and particulate impurities. Its coagulating and flocculating capabilities enable the removal of particles, inorganic and organic suspensions, and dissolved organic compounds.

In this study, photochemical polymerization was employed to synthesize poly(NVI-GMA). Characterization of the copolymer was carried out using UV-Visible spectroscopy, ^{1}H NMR, XRD, and FTIR techniques. The elimination analysis of Maghnite suspension turbidity was conducted to investigate the influence of various variables on the process, such as initial turbidity, pH of the aqueous medium, and flocculant concentration.

EXPERIMENTAL

Materials

The materials used in this work are N-Vinylimidazole (NVI) ($C_5H_6N_2$, 99%**,** Alfa Aesar), Glycidyl methacrylate (GMA) ($C_7H_{10}O_3$, biochem), Ammonium persulfate (APS)($(NH_4)_2S_2O_8$ biochem), chloridryic acid (HCl 37% biochem), and Maghnite (Clay material in its raw form from Maghnia Algeria [22])

Method of Copolymerization

The polymerization reaction involved using 50% (v/v) of each monomer and took place over a duration of 4 min. Ammonium persulfate (APS) was used as a 2% initiator, and 0.1 M hydrochloric acid (0.5 ml) was added to the quaternize NVI during synthesis. The polymerization process was conducted using a microwave reactor. Microwave polymerization was a chemical reaction induced by heat, ultraviolet (UV) radiation, or electron beam radiation. In this case, the thermal process was employed, utilizing metal molds and being well-suited for mass production. The reaction was carried out without the use of solvents since the two monomers were miscible with each other, and APS dissolved in the medium (see Fig. 1).

The resulting copolymer was washed with diethyl ether to remove any excess monomers. The medium was

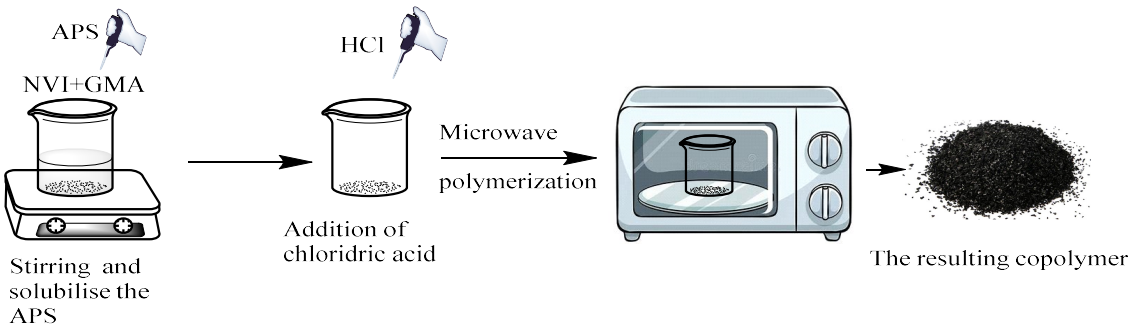

Fig. 1. The copolymerization method.

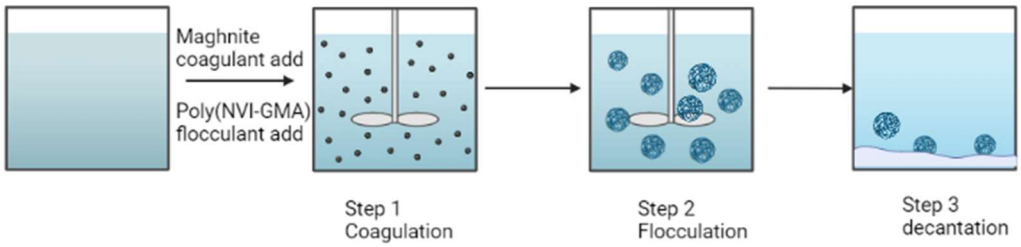

Fig. 2. Shows the Coagulation-flocculation process.

neutralized using ethanol, and the copolymer was then dried for 24 h at a temperature of 60 °C.

Characterization

Infrared spectra were recorded using an Agilent Technologies Cary 600 Series FTIR spectrometer. The copolymer sample was analyzed in powder form to qualitatively characterize the newly obtained functional groups.

X-ray diffraction measurements were performed using a Rikagu ultima IV (BD64000266-01) instrument. The samples were scanned over a 2° interval ranging from 5 to 60 degrees to obtain the poly(NVI-GMA) diffraction pattern. Thermogravimetric analysis (TGA) was conducted using a high-resolution TGA instrument (TA Instruments SDT Q600). The copolymers were thermally assessed from 50 to 650 °C at a heating rate of 10 °C min^{-1}.

The effective weight ratio of each modified monomer in the resulting copolymer was calculated using UV-visible spectrophotometry (Optizen 2120).

The point of zero charge (pH_{PZC}) was determined using the batch equilibrium method [23]. In this method, 30 ml of 0.01 M NaCl solutions were adjusted to a pH range of 2-12 using 0.1 M HCl or NaOH solutions. Each solution was then treated with 0.1 g of adsorbent. The suspensions were stirred at room temperature for 24 h, and the final pH of the solutions (pH_f) was determined to plot (pH_f-pH_i) against pH (pH_i) and determine the initial point of zero charge (pH_{PZC}).

The copolymer structure of poly(NVI-GMA) was evaluated using ^1H NMR analysis with the Bruker AV III spectrometer in $CDCl_3$ as the solvent.

Coagulation-flocculation Study

We prepared synthetic wastewater by mixing maghnite with distilled water. The flocculation studies were carried out using a jar-test apparatus, as depicted in Fig. 2. The initial turbidity (T_0) of the suspension was measured, and subsequently, the turbidity after adding different quantities of the flocculant (T_f) was determined using a turbidimeter (HI 93703). This measurement allowed us to evaluate the effectiveness of the flocculant. The percentage of turbidity removal was calculated using the following formula [15]:

$$\text{Turbidity removal } \% = \frac{(T_0 - T_f)}{T_0} \quad (1)$$

RESULTANTS AND DISCUSSIONS

UV-Visible Characterization

Aqueous solutions of copolymers and both monomers, all having the same concentration of 3×10^{-3} g ml^{-1}, were used to obtain the UV-Visible spectra shown in Fig. 3. The copolymer and NVI exhibited a distinct transition with a maximum wavelength around 290 nm, which can be attributed to the π-π* and σ-π* transitions of the C=N bond [24]. On the other hand, GMA displayed an absorption peak at approximately 300 nm, corresponding to the transition of the dioxide ring. The absorption peaks observed in the poly(PVI-GMA) copolymer, characterized by a broad band, represent a characteristic combination of NVI and GMA.

^{1}H NMR Characterization

The precursor of the synthesized poly(NVI-GMA) copolymer was characterized using ^{1}H NMR spectroscopy. In the ^{1}H NMR spectrum (Fig. 4), the methyl groups of GMA are observed as peaks at 1.2 ppm. The carbon skeletons of the copolymer are represented by peaks at 2.0 ppm, 2.6 ppm, and 3.7 ppm. Peaks at 3 and 4.2 ppm correspond to the protons of the ring dioxide [25]. The peaks at 6.7-7 ppm indicate the presence of imidazole ring protons. The quaternization proton of the ring NVI is represented by the final peak at 6.75 ppm.

The appearance of three groups of methine signals can be attributed to the presence of different tactility effects. The interpretation of peaks beyond isotactic and syndiotactic sequences is uncertain, although the central methine peak likely arises from protons at the heterotactic triads. The relative ratios of the three resonances indicate that this is primarily an atactic and alternative copolymer.

Determination of the pH_{PZC} of the Materials Used

The pH_{PZC} (point of zero charge) represents the pH value at which the surface of a substance carries no net charge. To determine the pH_{PZC}, the curve of $f(pH_i)$ and the axis pH_f-pH_i = 0 were plotted, and the point where they intersect the x-axis indicated its value. As shown in Fig. 5, poly(NVI-GMA) had a pH_{PZC} of 7.11, while Maghnite had a pH_{PZC} of 5.94.

When the pH of the solution was at pH_{PZC} values, the surfaces of these materials became positively charged, leading to anionic attraction. On the other hand, if the pH of the solution exceeds the pH_{PZC}, the surfaces become negatively charged and act as cation attractors.

During the optimization of coagulant and flocculant

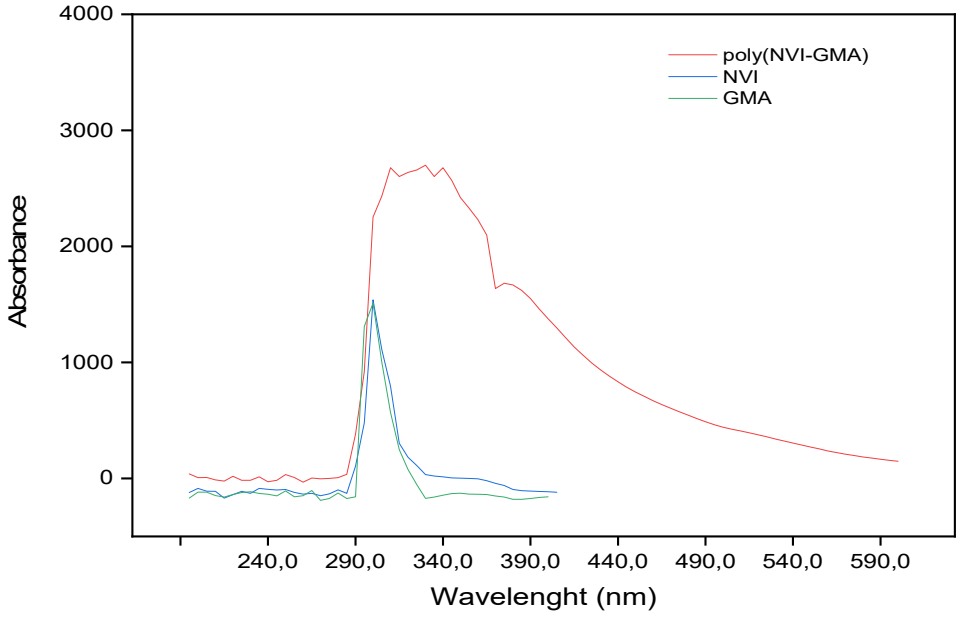

Fig. 3. UV-Visible spectrum.

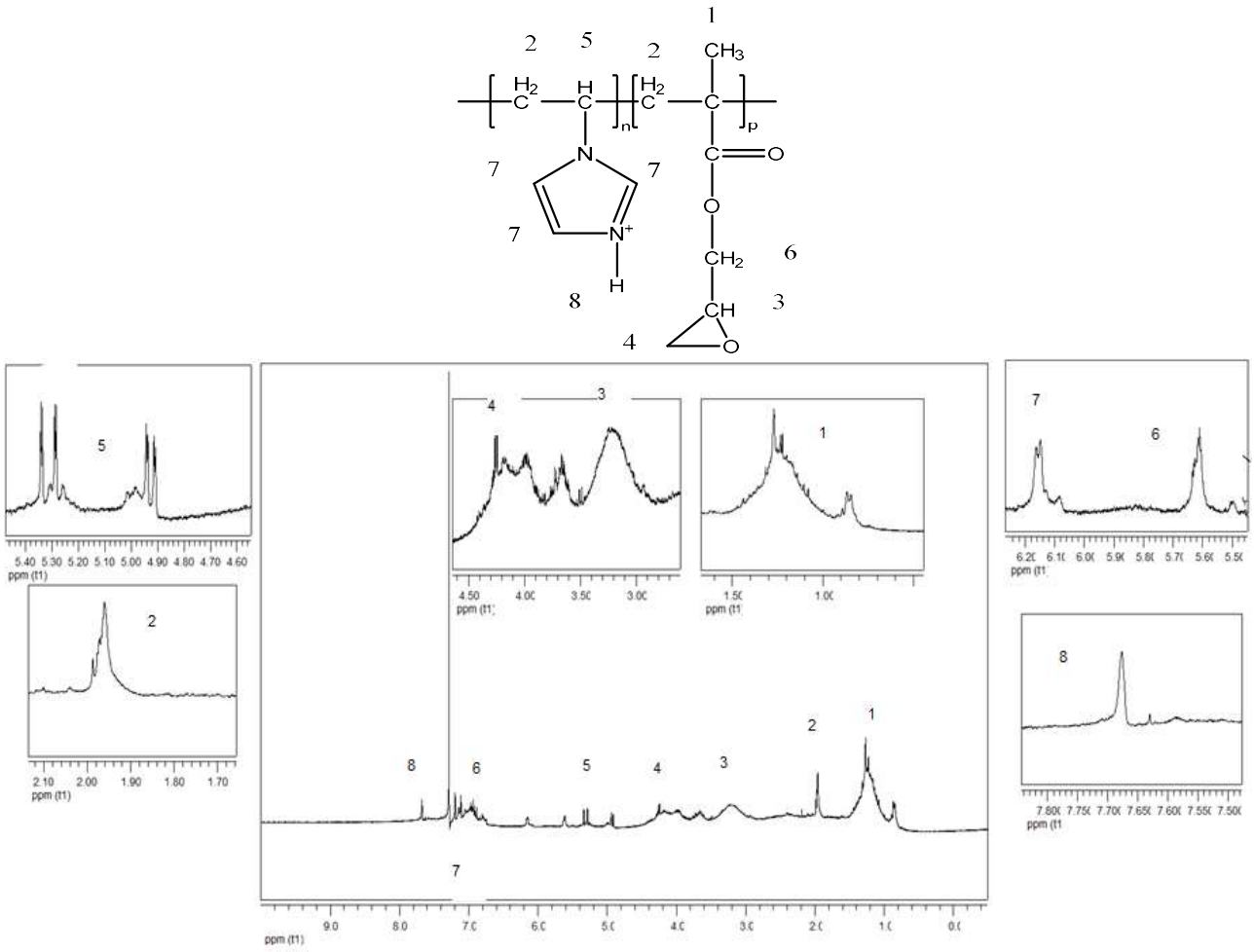

Fig. 4. The proposed copolymer structure and the ^{1}H NMR spectrum.

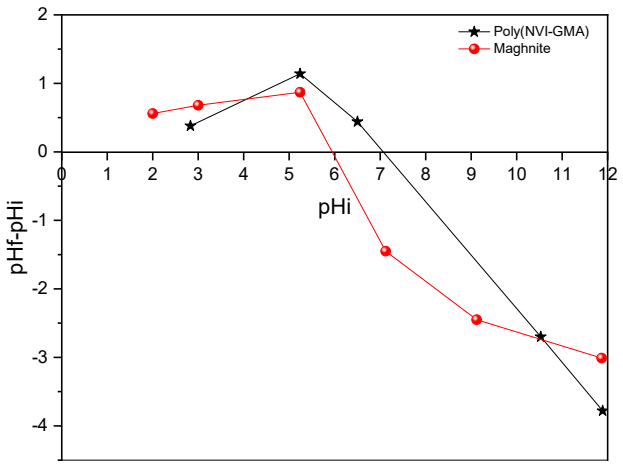

Fig. 5. Determination of pH_{PZC} of maghnite and poly(NVI-GMA).

weights, a pH of 6 was set, while other parameters were optimized within the pH range of 6 to 7 (neutral pH). By maintaining the pH of the solution within the range of 5.5-7.5, several advantages were achieved for both the environment and the economy. It eliminates the need for hazardous chemicals to adjust the pH to acidic or basic levels.

COAGULATION-FLOCCULATION PROCESS

Study of Maghnite Suspensions

To evaluate the removal of turbidity from maghnite suspensions through the coagulation-flocculation process, we initially examined the natural settling of maghnite at different starting concentrations and pH levels. Suspensions with

concentrations of 100, 200, 300, and 400 mg l^{-1} were carefully prepared in 1 l beakers by dispersing the appropriate amount of maghnite in distilled water. The residual turbidity was measured over a one-week settling period, and the percentage elimination of turbidity was calculated. The results are presented in Fig. 6.

The natural settling of maghnite was observed to be a gradual process, as depicted in Fig. 6. Based on the provided data, a maximum percentage elimination of 41% was achieved after two days of settling for a concentration of 100 mg l^{-1}. However, with the same maghnite suspension concentration (100 mg l^{-1}) and settling time (days), a maximum percentage elimination of 92% was obtained. This significant increase can be attributed to the presence of numerous suspended particles. The coagulation-flocculation process facilitates the rapid settling and accumulation of these particles. These findings indicate that highly turbid water settles naturally at a faster rate.

Removal of Turbidity by Flocculants Based on Synthesized Copolymers

pH effect. Figure 7 illustrates the relationship between turbidity removal and pH. The results indicate that the copolymers exhibit optimal performance in an acidic environment within the pH range of 2-3. Turbidity removal was less pronounced between pH 4 and pH 8, while the efficiency of the flocculant increased in the alkaline environment. These findings emphasize the significance of pH in the turbidity removal process and confirm that an acidic pH provides the best conditions for optimal performance.

The preference for an acidic environment can be attributed to the absence of positively charged sites, which are crucial for the charge neutralization technique employed to remove negatively charged Maghnite particles. The poly(NVI-GMA) copolymer demonstrates effective flocculation properties in acidic media. At a pH of 2.36 and a copolymer concentration of 20 mg l^{-1}, the turbidity removal efficiency reached 43.2%. This outcome is attributed to the adsorption of negatively charged Maghnite particles onto the positively charged nitrogen sites generated by the addition of HCl acid on the surface of the copolymer.

Figure 8 presents the destabilization mechanism of the coagulant, which can explain the combination of an acidic pH and a high percentage reduction in turbidity. When the copolymer was added to the Maghnite suspension, the negatively charged particles interacted with the positive charges present in the poly(NVI-GMA) structure, resulting in the creation of electrostatic (neutralized and negative)

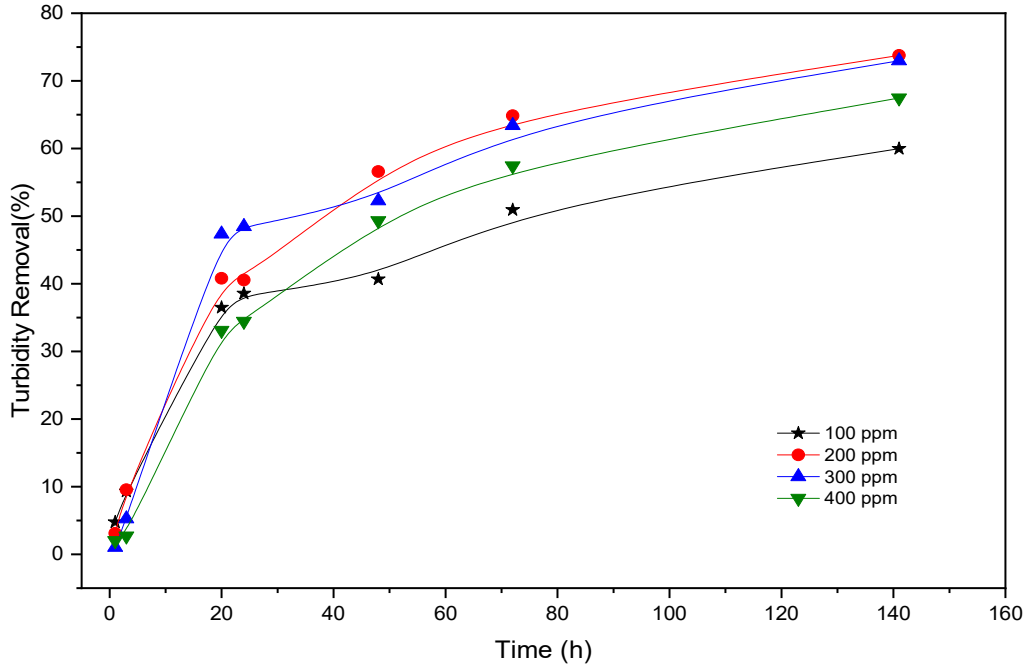

Fig. 6. The natural settling of maghnite.

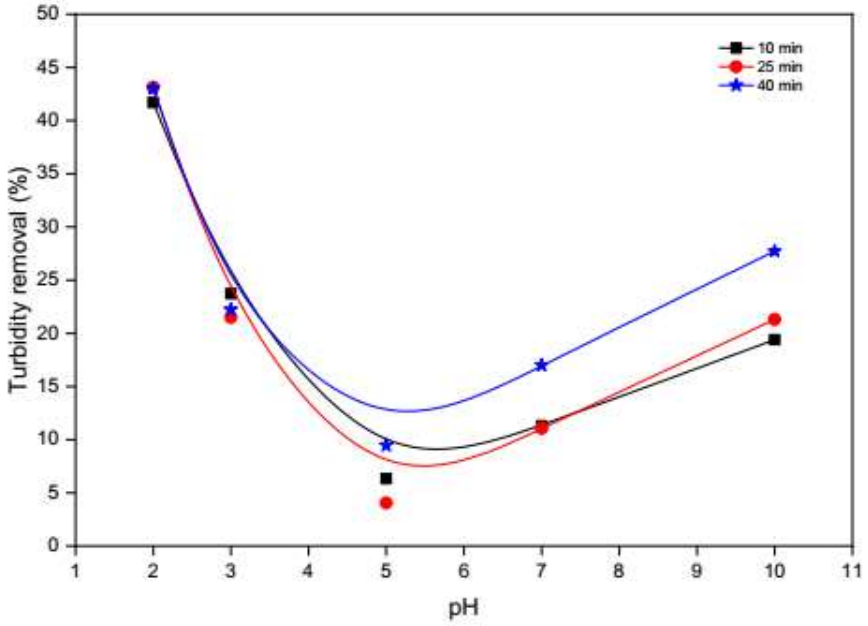

Fig. 7. Turbidity removal from Maghnite suspension ($C_{Maghnite}$ = 100 mg l^{-1}, Tu_0 = 27 NTU, $C_{copolymer}$ = 20 ppm) as function of pH with different settling time.

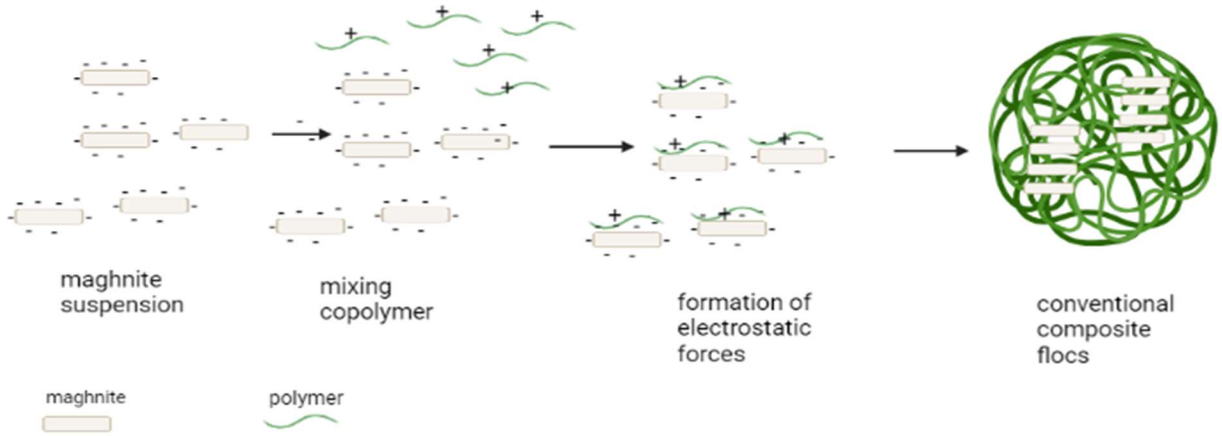

Fig. 8. proposed flocculation mechanism.

patches on the Maghnite particles. As a result, the numerous sites on the particles interacted with each other, forming microflocs that resemble typical composites. This electrostatic coagulation (ESP) process, facilitated by the addition of a low molecular weight destabilizing chemical, effectively removed turbidity from the solution by partially neutralizing the negative charge of the particles. Consequently, the treatment of the Maghnite suspension with poly(NVI-GMA) led to an unstable system with minimal residual turbidity and loose flocs, which is supported by XRD analysis.

Concentration effect of copolymers on turbidity removal. Figure 9 presents the efficiency of Maghnite turbidity removal as a function of flocculant concentration at different settling times. It was observed that an optimal turbidity elimination of 94.69% was achieved with a concentration of 6 ppm of the poly(NVI-GMA) flocculant.

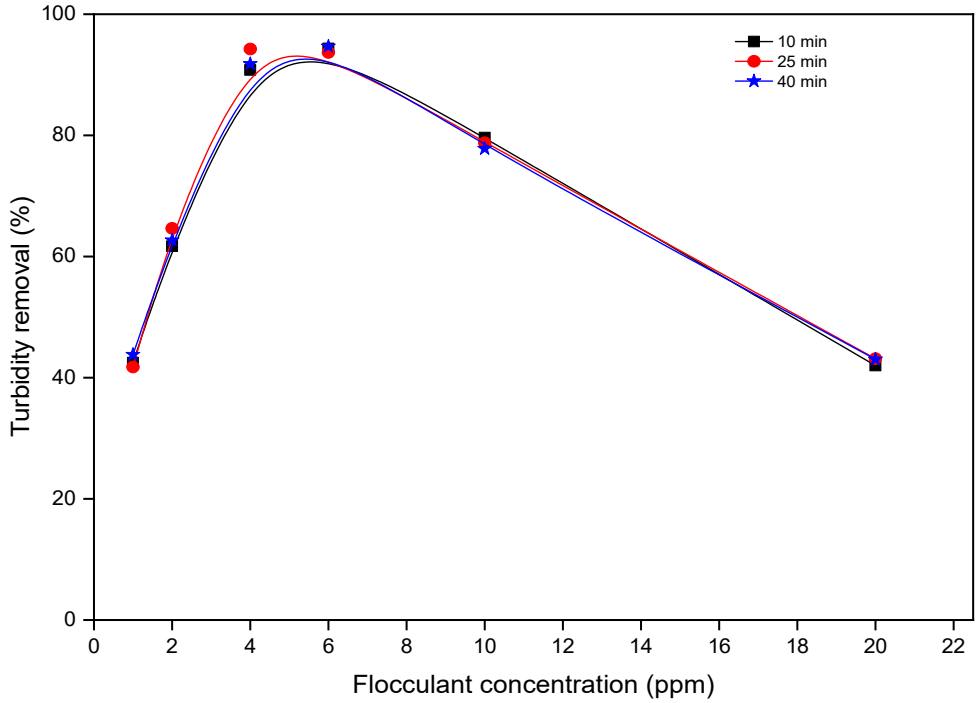

Fig. 9. Turbidity removal from Maghnite suspension ($C_{Maghnite}$ = 100 mg l^{-1}, Tu_0 = 27NTU, pH = 2.5) as function of flocculant concentration with different settling time.

The initial concentration of maghnite affected the optimal dosage of the copolymer, as shown in the graph.

To ensure optimal electrostatic contact between the ammonium groups of the NVI units and the negatively charged particles of Maghnite, a specific number of polymer chains was required. This explains the dependency on the initial maghnite concentration. Above the optimal concentration, the charged sites on the polymer chain became inaccessible to the Maghnite particles due to the high amount of polymer and significant intra-chain hydrogen interactions. As a result, the absorption of polymer particles by the Maghnite particles decreased.

Effect of coagulation speed and time on turbidity removal. The turbidity removal efficiency of a 100 mg l^{-1} Maghnite suspension was evaluated as a function of coagulation stirring speed, using the previously determined optimum concentration and pH. Figure 10 illustrates the results. It can be observed that the removal efficiency was improved as the stirring speed increased, reaching a maximum removal rate of 94.69% at a stirring speed of 200 rpm. However, beyond this value, the turbidity removal began to decrease. Hence, 200 rpm was identified as the ideal stirring speed for coagulation tests.

Figure 11 illustrates the relationship between turbidity removal and coagulation stirring time. Based on our observations, the highest removal value, reaching 97.05%, was achieved with 2 min of agitation. However, a good level of removal was also observed after 6 min of agitation followed by 40 min of standing. On the other hand, a decrease in turbidity removal was observed at 1 min and 4 min of stirring. Therefore, the optimal coagulation stirring time was determined to be 2 min.

Effect of flocculation speed and time on turbidity removal. Once the optimal flocculant concentration was determined, flocculation tests were conducted by keeping the dose constant while varying the stirring speed of the mixture for two minutes. The results are presented in Fig. 12a. Using the established optimal flocculant concentration, the removal of turbidity from the 100 mg l^{-1} maghnite suspension was evaluated as a function of stirring speed. The findings in Fig. 12a indicate that the removal efficiency remained stable up to an agitation speed of 30 rpm, after which it started to

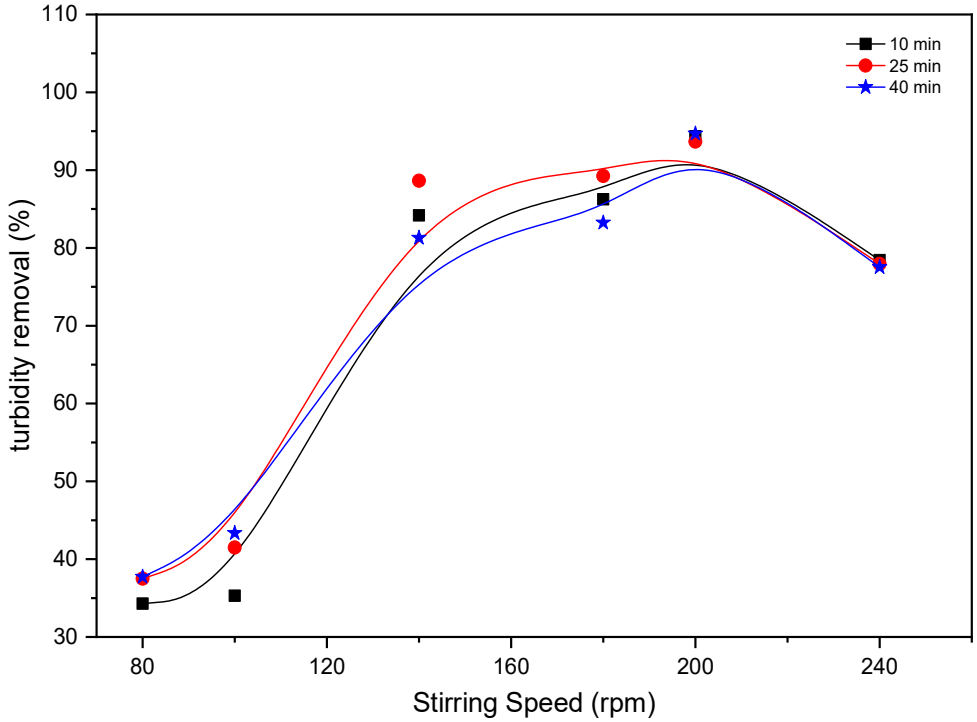

Fig. 10. Turbidity removal as a function of stirring speed for, $C_{copolymer}$ = 6 mg l^{-1}, and pH = 2.5.

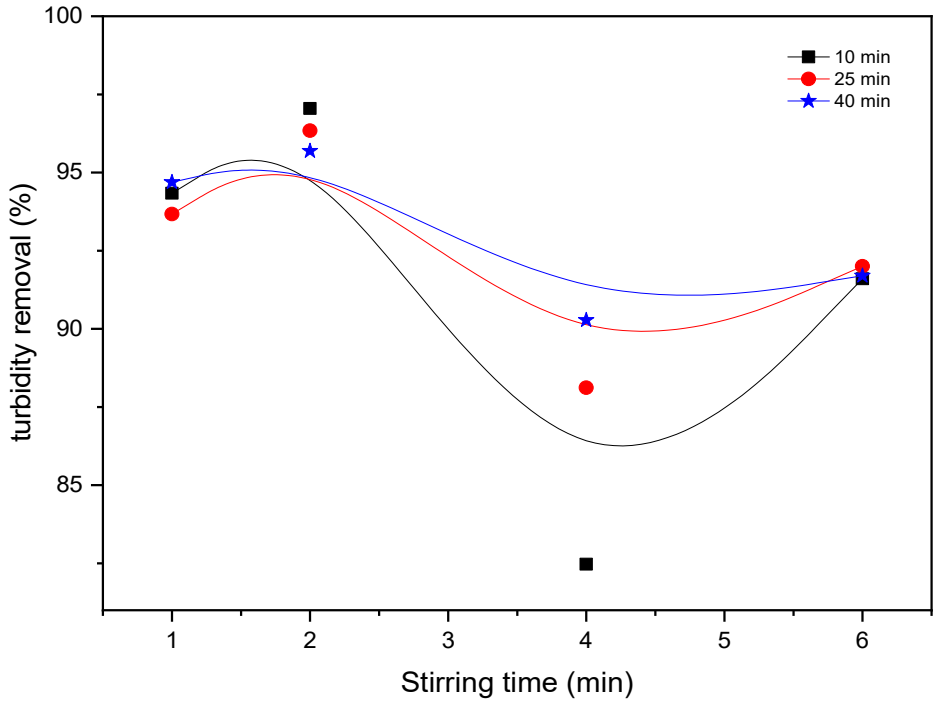

Fig. 11. Turbidity removal as a function of stirring time under 200 rpm with the optimum dose of flocculant with $C_{Maghnite}$ = 100 mg l^{-1}, Tu_0 = 27 NTU, pH = 2.5, $C_{copolymer}$ = 6 mg l^{-1}.

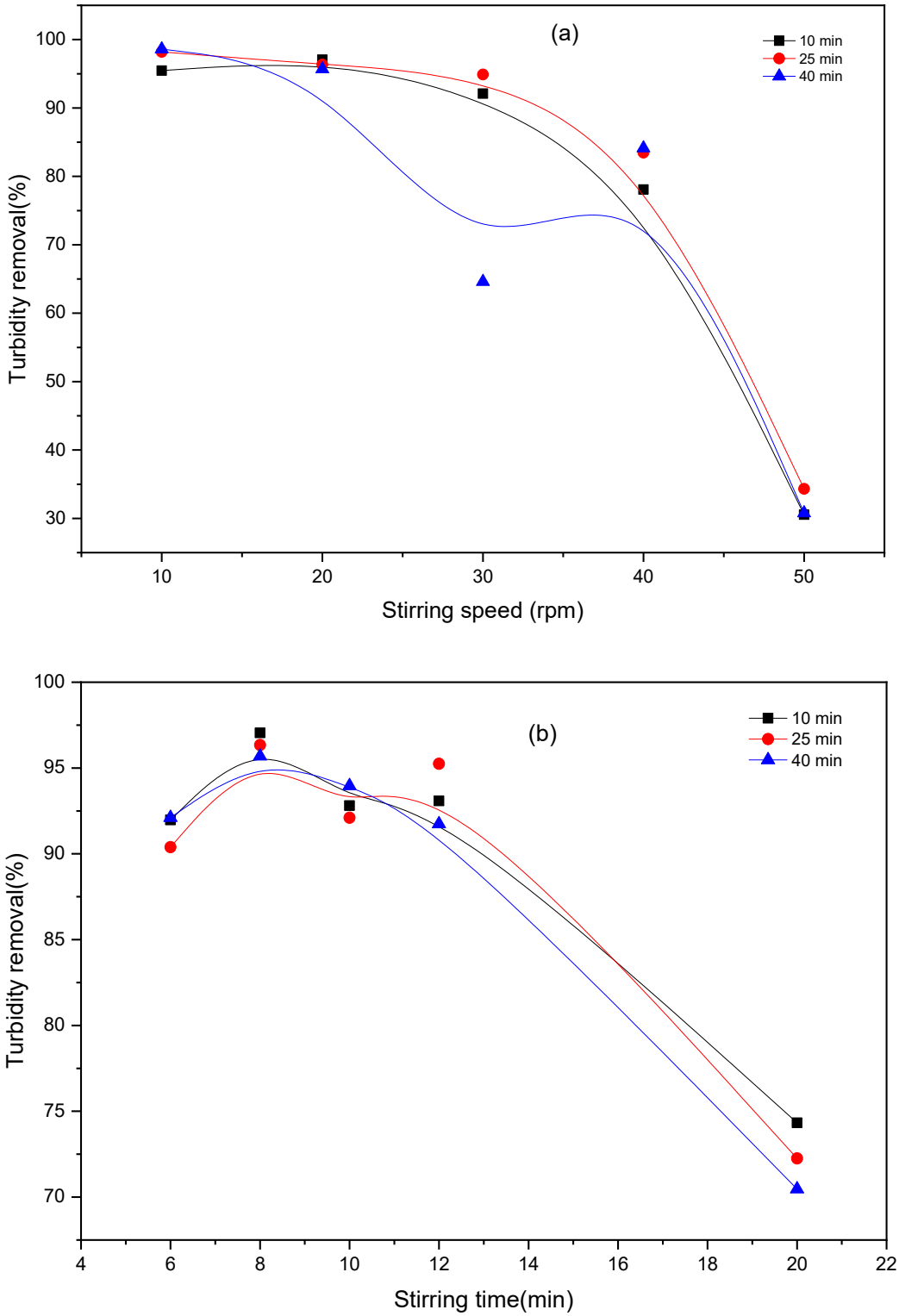

Fig. 12. Effect of flocculation a speed and b time on turbidity removal ($C_{copolymer}$ = 6 mg l^{-1}, pH = 2.5, $C_{Maghnite}$ = 100 mg l^{-1}, Tu_0 = 27 NTU).

decrease with the flocculant. The ideal stirring speed for flocculation testing was determined to be 20 rpm.

Furthermore, flocculation tests were carried out to determine the optimal stirring duration by adjusting the stirring time while maintaining the optimal flocculant concentration and setting the stirring speed at 20 rpm (Fig. 12b). The results of the various experiments are displayed in Fig. 12b. The effectiveness of turbidity removal was calculated as a function of the optimal flocculant concentration, stirring time at 20 rpm, and both factors combined. The findings demonstrate that flocculation efficiency increased for up to 8 min of flocculant agitation. However, the tested flocculant showed a decline in efficiency after 8 min.

The turbidity elimination of poly(NVI-GMA) was therefore as high as that of other materials in functional studies, according to our work and the comparison with other works (Table 1). However, this study focuses not only on the percentage of turbidity elimination, but also on the reduction of other parameters such as time and speed.

FTIR CHARACTERIZATION

The FTIR spectrum of poly(NVI-GMA) (Fig. 13) exhibited seven prominent peaks at specific wavenumbers. These peaks and their corresponding functional groups are as follows:

Table 1.

Flocculants	Coagulant mass (mg l^{-1})	Coagulation speed (rpm)	Coagulation time (min)	Flocculation speed (rpm)	Flocculation time (min)	Removal (%)
Poly(NVI-GMA)	100	200	2	20	8	97.05
AD37-PPD [15]	100	120	2	50	10	95.67
AM-VP-0.5% [3]	100	100	0.5	50	4	89.3
Yeast cell wall [1]	300	100	1	50	15	97

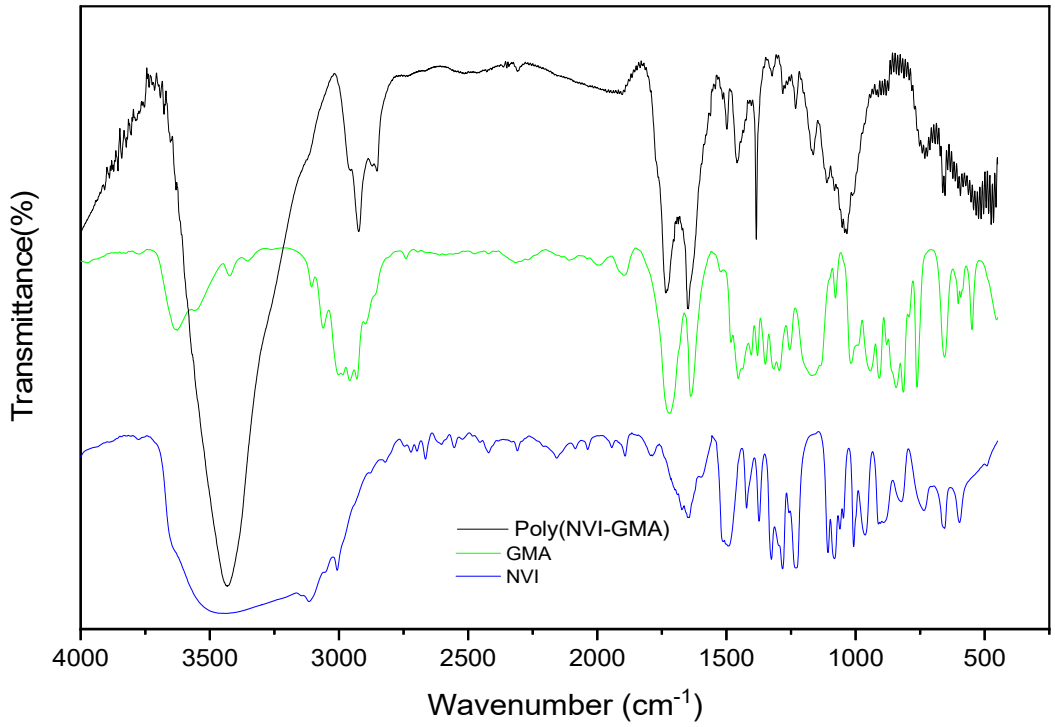

Fig. 13. FTIR spectrum of copolymer and maghnite and the flocs obtained.

Peaks at 3326 cm^{-1} and 2934 cm^{-1}: These peaks are attributed to absorbed water and C-H ring stretching, respectively.

Peak at 1226 cm^{-1}: This peak indicates C-N ring stretching.

Peak at 750 cm^{-1}: This peak represents C-N ring stretching and chain bending [26], which are characteristic of NVI as the monomer.

Peak at 661 cm^{-1}: This peak indicates Copolymer ring twisting, further confirming the presence of NVI in the copolymer.

In addition to the NVI-specific peaks, there are characteristic peaks associated with GMA and the copolymerization process:

Peak at 1724 cm^{-1}: This peak corresponds to C=O stretching vibration, indicating the presence of carbonyl groups in the copolymer.

Peaks at 1160 cm^{-1} and 1388 cm^{-1}: This peak represents C-O-C stretching, and -CH3 respectively, which indicates the presence of ether linkages in the copolymer.

Peak at 905 cm^{-1}: This peak is assigned to the epoxy ring, suggesting the incorporation of epoxy groups in the copolymer [27]. The peak at 2956 cm^{-1} represents the C-H bond.

Absence of peak at 1637 cm^{-1}: This absence indicates the successful copolymerization of GMA with NVI, as the peak at 1637 cm^{-1} represents the C=C stretching vibration in GMA.

The FTIR spectrum also revealed information about the maghnite and floc used in the coagulation process:

Peaks at 783 cm^{-1} and 1120 cm^{-1}: These peaks are assigned to Si-O and Si-O-Si vibrations, respectively, indicating the presence of silicon-oxygen bonds in maghnite.

The absence of new peaks in the floc spectrum suggests that no chemical reaction occurred during the coagulation process, indicating that no new functional groups were formed.

Furthermore, the absorption peaks at 3412 cm^{-1} and 1724 cm^{-1} in the floc spectrum are attributed to C-H stretching vibration and C=O stretching in the amide groups, respectively. However, these two peaks were the only ones present in the floc spectrum, likely due to the copolymer dosage being lower than the maghnite particle content in water.

THERMOGRAVIMETRIC CHARACTERIZATION

The thermal stability of the samples, including flocs, Poly(NVI-GMA), and Maghnite, was analyzed using thermogravimetric analysis (TGA). The results are shown in Fig. 14.

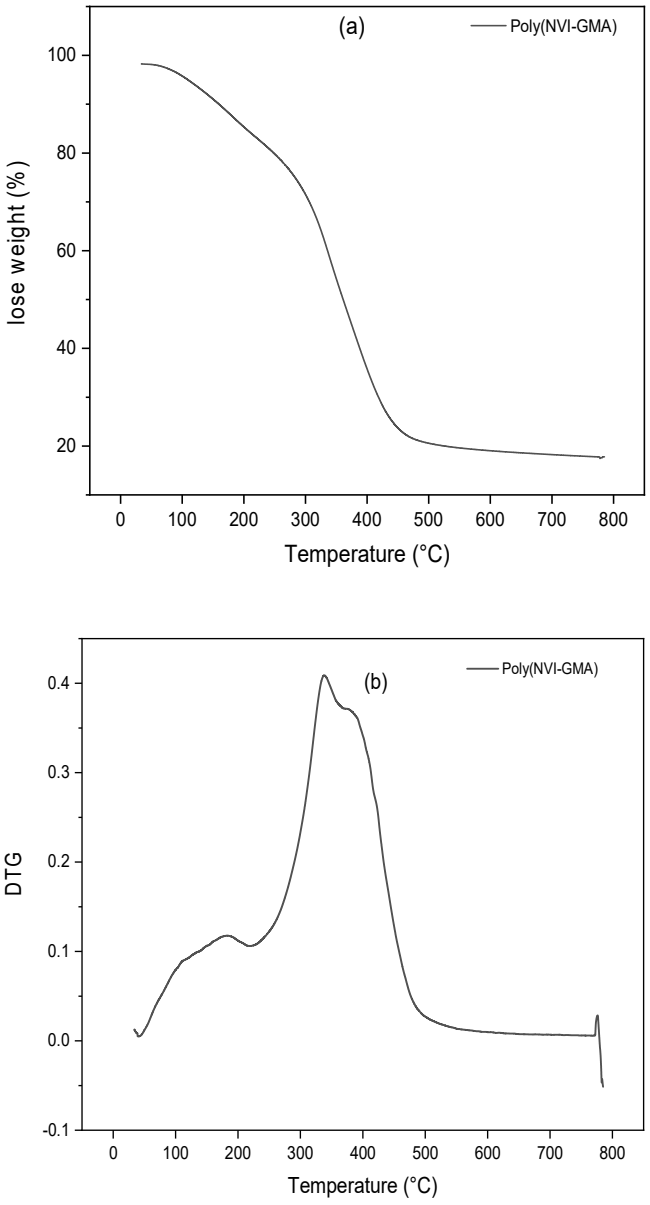

Fig. 14. a) Thermogravimetric curves and b) DTG curves for different materials.

From Fig. 14a, it was observed that the thermal stability of flocs increased with the nitrogen group concentration. The onset of weight loss occurred at around 370 °C. On the other hand, poly(NVI-GMA) exhibited a weight loss process starting at approximately 217 °C.

Figure 14b illustrates the degradation process for poly(NVI-GMA) and Maghnite. Poly(NVI-GMA) showed a broad peak, indicating a one-step degradation process. The degradation temperature for NVI and GMA was similar, occurring at around 343 °C. Maghnite, on the other hand, exhibited a two-step degradation process. The degradation temperature for Maghnite was predominantly observed in the range of 628 °C. The first weight loss, occurring at around 390 °C, corresponded to the degradation of the flocs. The second weight loss, between 600 and 630 °C, could be attributed to the degradation of Maghnite.

It is worth noting that the decrease in weight observed between 50 and 150 °C was likely due to the degradation of solvents used during the analysis.

These findings provide insights into the thermal stability of the samples and their respective degradation processes at elevated temperatures.

DRX CHARACTERIZATION

The X-ray diffractograms presented in Fig. 15 show the patterns for the copolymer, maghnite, and the composite material in the 2°-80° range. The copolymer exhibited an amorphous morphology, as indicated by the absence of distinct peaks in its XRD pattern [28].

The XRD pattern of the original maghnite showed a peak at 7.11°, representing its characteristic structure. However, in the composite material, this peak shifted towards 5.3°. This shift indicates a significant opening of the maghnite lamellae, which corresponds to an increase in interlayer spacing from 13.8 Å to 15.35 Å.

Based on these observations, it is postulated that the intercalated comonomers exert pressure on the montmorillonite gallery structure of maghnite, leading to the disintegration of the structure. This disintegration results in the formation of a typical composite material during the polymerization process.

The XRD results, along with the findings from FTIR spectroscopy, support the development of a well-defined structure for the conventional composite material.

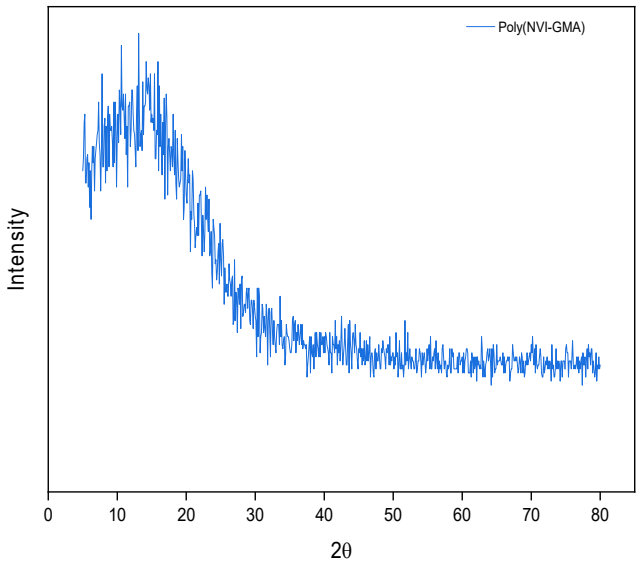

Fig. 15. DRX curves for different materials.

CONCLUSION

The microwave radical copolymerization process was utilized to synthesize copolymers with equal amounts of NVI and GMA monomers, resulting in high macromolecular weight copolymers. Various characterization techniques, including UV-Visible spectroscopy, FTIR spectroscopy, X-ray diffraction (XRD), ^{1}H NMR spectroscopy, and thermogravimetric analysis (ATG) were employed to investigate the copolymer's structure, adsorption properties, and thermal stability. The viscosity measurement was used to determine the weight of the macromolecules.

The primary focus of the study was to explore the potential application of the synthesized copolymers in wastewater treatment by investigating their flocculation behavior using maghnite as a coagulant. Comparative analysis revealed that poly(NVI-GMA) exhibited superior flocculation performance compared to other flocculants. The flocculation efficiency was recorded to be greater than 96% when optimal copolymer concentrations were employed for turbidity removal.

Several parameters were identified as influential factors affecting flocculation efficiency. These include the method

used for flocculation, the pH of the flocculant solution, stirring speed, and the duration of the flocculation step. These parameters were carefully considered and optimized to achieve the highest flocculation efficiency.

REFERENCES

[1] Ferasat, Z.; Panahi, R.; Mokhtarani, B., Natural polymer matrix as safe flocculant to remove turbidity from kaolin suspension: Performance and governing mechanism. *J. Environ. Manage*. **2020**, *255*, 109939, DOI: 10.1016/j.jenvman.2019.109939.

[2] Okolo, B. I.; Adeyi, O.; Oke, E. O.; Agu, C. M.; Nnaji, P. C.; Akatobi, K. N.; Onukwuli, D. O., Coagulation Kinetic Study and Optimization Using Response Surface Methodology for Effective Removal of Turbidity from Paint Wastewater Using Natural Coagulants. *Sci. African* **2021**, *14*, DOI: 10.1016/j.sciaf.2021.e00959.

[3] Hocine, T.; Benhabib, K.; Bouras, B.; Mansri, A., Comparative Study Between New Polyacrylamide Based Copolymer Poly(AM-4VP) and a Cationic Commercial Flocculant: Application in Turbidity Removal on Semi-Industrial Pilot. *J. Polym. Environ.* **2018**, *26*, 1550-1558, DOI: 10.1007/s10924-017-1049-7.

[4] Saritha, V.; Srinivas, N.; Srikanth Vuppala, N. V., Analysis and Optimization of Coagulation and Flocculation Process. *Appl. Water Sci.* **2017**, *7*, 451-460, DOI: 10.1007/s13201-014-0262-y.

[5] Okolo, B. I.; Nnaji, P. C.; Menkiti, M. C.; Onukwuli, O. D., A Kinetic Investigation of the Pulverized Okra Pod Induced Coag-Flocculation in Treatment of Paint Wastewater. *Am. J. Anal. Chem.* **2015**, *6*, 610-622, DOI: 10.4236/ajac.2015.67059.

[6] Amosa, M. K.; Jami, M. S.; Alkhatib, M. F. R., Electrostatic Biosorption of COD, Mn and H_2S on EFB-Based Activated Carbon Produced through Steam Pyrolysis: An Analysis Based on Surface Chemistry, Equilibria and Kinetics. *Waste and Biomass Valorization* **2016**, *7*, 109-124, DOI: 10.1007/s12649-015-9435-7.

[7] Tonhato Junior, A.; Hasan, S. D. M.; Sebastien, N. Y., Optimization of Coagulation/Flocculation Treatment of Brewery Wastewater Employing Organic Flocculant Based of Vegetable Tannin. *Water. Air. Soil Pollut*. **2019**, *230* (8), DOI: 10.1007/s11270-019-4251-5

[8] Baghvand, A.; Zand, A. D.; Mehrdadi, N.; Karbassi, A., Optimizing coagulation process for low to high turbidity waters using aluminum and iron salts. Am. *J. Environ. Sci*. **2010**, *6* (5), 442-448, DOI: 10.3844/ajessp.2010.442.448.

[9] Lin, J. C. T.; Wu, C. -Y.; Chu, Y. -L.; Huang, W. -J., Effects of High Turbidity Seawater on Removal of Boron and Transparent Exopolymer Particles by Chemical Oxo-Precipitation. *J. Taiwan Inst. Chem. Eng.* **2019**, *94*, 109-118, DOI: 10.1016/j.jtice.2018.02.012.

[10] Azimi, S. C.; Shirini, F.; Pendashteh, A., Evaluation of COD and Turbidity Removal from Woodchips Wastewater Using Biologically Sequenced Batch Reactor. *Process Saf. Environ. Prot.* **2019**, *128*, 211-227, DOI: 10.1016/j.psep.2019.05.043.

[11] Li, K.; Han, M.; Xu, Y.; Zhang, J.; Wei, T.; Wen, G.; Huang, T., Performance of Gravity-Driven Membrane Filtration for Treatment of Low-Temperature and Low-Turbidity Water: Effect of Coagulation Pretreatment. *J. Water Process Eng.* **2023**, *53*, 103782, DOI: 10.1016/j.jwpe.2023.103782.

[12] Iqbal, A.; Jalees, M. I.; Farooq, M. U.; Cevik, E.; Bozkurt, A., Superfast Adsorption and High-Performance Tailored Membrane Filtration by Engineered Fe-Ni-Co Nanocomposite for Simultaneous Removal of Surface Water Pollutants. *Colloids Surfaces A Physicochem. Eng. Asp.* **2022**, *652*, 129751, DOI: 10.1016/j.colsurfa.2022.129751.

[13] Wang, H.; Yang, Y.; Zhou, Z.; Li, X.; Gao, J.; Yu, R.; Li, J.; Wang, N.; Chang, H., Photocatalysis-Enhanced Coagulation for Removal of Intracellular Organic Matter from Microcystis Aeruginosa: Efficiency and Mechanism. *Sep. Purif. Technol.* **2022**, *283*, 120192, DOI: 10.1016/j.seppur.2021.120192.

[14] Chen, Y.; Xu, W.; Zhu, H.; Wei, D.; He, F.; Wang, D.; Du, B.; Wei, Q., Effect of Turbidity on Micropollutant Removal and Membrane Fouling by MIEX/Ultrafiltration Hybrid Process. *Chemosphere* **2019**, *216*, 488-498, DOI: 10.1016/j.chemosphere.2018.10.148.

[15] Bouras, B.; Hocine, T.; Benhabib, K.; Zair, R.; Mansri,

A.; Tennouga, L.; Guemra, K., Turbidity Removal from Bentonite Suspension by Coagulation/Flocculation Using Modified p-Phenylenediamine/ Poly(Acrylamide). *Rev. Roum. Chim.* **2019**, *64*, 985-991, DOI: 10.33224/rrch.2019.64.11.07.

[16] Kumari, M.; Gupta, S. K., A novel process of adsorption cum enhanced coagulation-flocculation spiked with magnetic nanoadsorbents for the removal of aromatic and hydrophobic fraction of natural organic matter along with turbidity from drinking water. *J. Clean. Prod*. **2020**, *244*, 118899, DOI: 10.1016/ j.jclepro.2019.118899.

[17] Abdollahi, K.; Yazdani, F.; Panahi, R., Covalent immobilization of tyrosinase onto cyanuric chloride crosslinked amine-functionalized superparamagnetic nanoparticles: Synthesis and characterization of the recyclable nanobiocatalyst. *Int. J. Biol. Macromol*. **2017**, *94*, 396-405, DOI: 10.1016/ j.ijbiomac.2016.10.058.

[18] Belkaid, S.; Mahroug, H.; Zennaki, M. el A.; Tennouga, L., Removal of Acid Blue 113 Textile Dye from Synthetic Aqueous Solution by Adsorption and Flocculation Process Using Cationic Copolymer Poly(n-Hexadecyl-4-Vinylpyridinium Bromide). *Phys. Chem. Res.* **2024**, *12*, 61-72, DOI: 10.22036/ pcr.2023.383952.2279.

[19] Lee, C. S.; Robinson, J.; Chong, M. F., A Review on Application of Flocculants in Wastewater Treatment. *Process Saf. Environ. Prot.* **2014**, *92*, 489-508, DOI: 10.1016/j.psep.2014.04.010.

[20] Benaglia, M.; Alberti, A.; Giorgini, L.; Magnoni, F.; Tozzi, S., Poly(Glycidyl Methacrylate): A Highly Versatile Polymeric Building Block for Post-Polymerization Modifications. *Polym. Chem.* **2013**, *4*, 124-132, DOI: 10.1039/c2py20646c.

[21] Palenzuela, M.; Valenzuela, L.; Amariei, G.; Vega, J. F.; Mosquera, M. E. G.; Rosal, R., Poly(Glycidyl Methacrylate) Macromolecular Assemblies as Biocompatible Nanocarrier for the Antimicrobial Lysozyme. *Int. J. Pharm.* **2021**, *603*, 120695, DOI: 10.1016/j.ijpharm.2021.120695.

[22] Benadda, M.; Ferrahi, M. I.; Belbachir, M., Synthesis of Poly(N-Vinyl-2-Pyrrolidone-Co-Methyl Methacrylate) by Maghnite-H+ a Non-Toxic Catalyst. *Bull. Chem. React. Eng. & amp;amp; Catal.* **2014**, *9*, 201–206, DOI: 10.9767/bcrec.9.3.5743.201-206.

[23] Snik, A.; Jioui, I.; Larzek, M.; Assabbane, A.; Zahouily, M., Cationic Dye Removal (Methylene Blue) from Aqueous Solution Using the Ecologically Friendly Alginate/Hydroxyapatite/Graphene Oxide Nanocomposite Hydrogel Beads. *Water. Air. Soil Pollut.* **2022**, *233*, DOI: 10.1007/s11270-022-05747-x.

[24] Wang, X.; Wang, D.; Guo, Y.; Yang, C.; Iqbal, A.; Liu, W.; Qin, W.; Yan, D.; Guo, H., Imidazole Derivative-Functionalized Carbon Dots: Using as a Fluorescent Probe for Detecting Water and Imaging of Live Cells. *Dalt. Trans.* **2015**, *44*, 5547-5554, DOI: 10.1039/ c5dt00128e.

[25] Cheng, Y. -L.; Wong, R. -J.; Lin, J. C. -T.; Huang, C.; Lee, D. -J.; Mujumdar, A.S., Water Coagulation Using Electrostatic Patch Coagulation (EPC) Mechanism. *Dry. Technol.* **2010**, *28*, 850-857, DOI: 10.1080/07373937.2010.490492.

[26] Nor Fadzil, N. F. E.; Abouzari-Lotf, E.; Jacob, M. V.; Che Jusoh, N. W.; Ahmad, A., Surface-Modified Fibrous Membranes for Fuel Cell Application. *E3S Web Conf.* **2019**, *90*, 01005, DOI: 10.1051/e3sconf/ 20199001005.

[27] Saikia, B. J.; Dolui, S. K., Designing Semiencapsulation Based Covalently Self-Healable Poly(Methyl Methacrylate) Composites by Atom Transfer Radical Polymerization. *J. Polym. Sci. Part A Polym. Chem.* **2016**, *54*, 1842-1851, DOI: 10.1002/ pola.28046.

[28] M.El Amine, Z.; Lahcene, T.; Brahim, B.; Kouider, M., Methods of Recycling Expanded Polystyrene Waste: Synthesis and Characterization. *Phys. Chem. Res*. **2023**, *11* (4), 943-951, DOI: 10.22036/pcr.2023.365735.2220.